

IDENTIFICATION OF A GLOBAL ANEUPLOIDY-ASSOCIATED
TRANSCRIPTIONAL AND PHENOTYPIC SIGNATURE IN BUDDING YEAST

by
Anjali Nelliat

A thesis submitted to Johns Hopkins University in conformity with the requirements
for the degree of Master of Science in Engineering

Baltimore, Maryland

May, 2017

Abstract

Aneuploidy, an unbalanced genome state with either gain or loss of chromosomes, is known to have dramatic effects on cellular physiology, ranging from detrimental effects including genetic disorders such as Down Syndrome to promoting adaptability under stress, such as drug resistance. This paradoxical nature of aneuploidy impedes the development of therapeutic strategies since a vast majority of tumors exhibit complex aneuploid karyotypes. Although the aneuploid cancer genome has been extensively studied, common transcriptional and phenotypic consequences of aneuploidy still remain elusive. To comprehensively study aneuploidy-specific features, we first generated karyotypically heterogeneous aneuploid populations in budding yeast *Saccharomyces cerevisiae*, based on our general statistical model. We then performed whole transcriptome sequencing on these heterogeneous aneuploid populations, to uncover a karyotype-independent, global aneuploidy-associated transcriptional response. The aneuploid transcriptome was similar to gene expression profiles of yeast cells subject to hypo-osmotic and cell-wall stresses. Furthermore, we observed that aneuploid cells indeed exhibited phenotypes characteristic of these stresses, including cell swelling, increased glycerol efflux, lower intracellular viscosity and a compromised cell wall. Finally, we also observed a significant reduction in endocytosis in the aneuploid population, resulting in perturbed cellular homeostasis. Interestingly, decreasing the effective turgor pressure by addition of sorbitol rescued the endocytosis defect. Thus, our results shed light on novel cellular consequences of aneuploidy that can be further studied to reveal detailed molecular mechanisms in aneuploidy and identify new potential targets for anticancer therapeutics.

(Advisor: Dr. Rong Li **Reader:** Dr. Michael Schatz)

Acknowledgements

During the course of this project, I have had the good fortune of being surrounded by people who have been invaluable with their advice and encouragement. First, I would like to thank my advisor, Dr. Rong Li, for giving me the opportunity to work on this exciting project as well as for being a truly inspirational scientific role model.

I am incredibly grateful to Dr. Hung-Ji Tsai, the best mentor I could have possibly imagined. Thank you for the unwavering patience and countless hours you have put into teaching and helping me, and for sharing your knowledge of science and life that has helped me grow as both a scientist and a person.

I am thankful to Dr. Michael Schatz for training me in computational genomics, a field I have come to love, and guiding me as I applied it during the course of this project. Thank you also for agreeing to be a part of my thesis committee.

The Rong Li lab provides a great scientific environment with a truly collaborative spirit. I thank all the members of the lab for their help and camaraderie.

Finally, I'm immensely grateful to my family and friends. Thank you Safwan and Neetu, for those lengthy Skype conversations despite conflicting time zones. To my parents, thank you for your unrelenting support as well as encouraging the curiosity and creativity that led me to pursue science.

Table of Contents

Introduction	1
Mechanisms that cause aneuploidy	1
Consequences of aneuploidy	4
<i>Effects of aneuploidy on gene expression</i>	4
<i>Phenotypes associated with aneuploidy</i>	5
The role of aneuploidy in cancer	7
<i>Saccharomyces cerevisiae</i> as a model system to study aneuploidy	8
Aim of Research	9
Materials and Methods	11
Yeast strains and growth condition	11
Statistical model for determination of aneuploid population size	12
<i>Model assumptions</i>	12
<i>Mathematical design</i>	12
Next Generation Sequencing (NGS) data analysis pipeline	13
<i>Data pre-processing and quality control</i>	13
<i>Copy number analysis</i>	14
<i>Transcriptome analysis</i>	14
Comparison of transcriptome results to published datasets	15
Monitoring cell swelling	16
Measurement of glycerol concentrations	16
Intracellular viscosity assay	17
Endocytosis assays	17
Zymolyase sensitivity assay	18
Statistical Analysis	18
Results	19
Generation of aneuploid populations with uniform ploidy distribution	19
Identification of an aneuploidy driven stress response	25
<i>Aneuploid population transcriptome resembles transcriptional signatures of cells under</i> <i>hypo-osmotic shock and cell wall stress.</i>	25
<i>Aneuploidy stress does not correlate with ESR induction.</i>	26
Phenotypic consequences of the aneuploidy stress response	29
<i>Aneuploid cells exhibit excessive cell swelling</i>	29
<i>Aneuploid cells possess lower bulk intracellular viscosity</i>	32
<i>Aneuploid cells display increased sensitivity to zymolyase</i>	34
<i>Endocytosis is reduced in aneuploid cells</i>	35
Discussion	39
References	44
Curriculum Vitae	47

List of Figures

Figure 1: The attachment process during chromosome segregation	3
Figure 2: Aneuploidy confers phenotypic variation under diverse stresses	7
Figure 3: Triploid meiosis gives rise to aneuploid progenies.....	10
Figure 4: Model estimation of aneuploid population ploidy distribution.....	21
Figure 5: Aneuploid populations display uniform ploidy.	24
Figure 6: Transcriptome analysis of aneuploid populations.	15
Figure 7: Comparison of the aneuploidy transcriptome to published gene expression profiles.....	28
Figure 8: Aneuploid cells exhibit hypo-osmotic cell swelling.....	31
Figure 9: Extracellular and intracellular glycerol concentrations are altered in aneuploid cells.	32
Figure 10: Bulk intracellular viscosity is shifted in aneuploid populations.	34
Figure 11: Aneuploidy enhances zymolyase sensitivity.....	35
Figure 12: Endocytosis is decreased in aneuploid cells.	38

List of Tables

Table 1.1 : Mean chromosome copy number of aneuploid populations	22
Table 1.2: Copy number variants in euploid or aneuploid populations.....	2

Introduction

A balanced genomic state with a karyotype that is an exact multiple of the haploid genome content is termed euploidy. Divergence from euploidy, such that one or more chromosomes possess an excess or reduced copy number results in a genome state called aneuploidy. Across species, aneuploidy is known to have diverse consequences on organismal fitness, viability and reproduction. Aneuploidy is also associated with several genetic disorders and human diseases, including cancer. As work presented in this thesis will show, aneuploidy can have a profound global effect at the transcriptome level which can lead to drastic phenotypic consequences in budding yeast *Saccharomyces cerevisiae*, and potentially, higher organisms.

This introduction briefly reviews the mechanisms that might induce aneuploidy and its known downstream consequences on cell physiology. Following this, the role of aneuploidy in cancer is addressed, and finally, the potential of *S. cerevisiae* as a model organism to study the global effects of aneuploidy is discussed.

Mechanisms that cause aneuploidy

During both meiotic and mitotic cell division, accurate segregation of duplicate chromosomes is necessary to preserve integrity of the genome. Errors in chromosome segregation leads to unequal partitioning of the chromosomes and results in generation of aneuploid cells (Musacchio and Salmon 2007). There are few possible mechanisms by which chromosome missegregation can occur (Cimini, et al. 2001) (Musacchio and Salmon 2007) (Thompson and Compton 2011). During a normal mitotic division, chromosomes condense during prophase, and protein complexes known as kinetochores assemble on the

centromeres of each of the chromatids on the chromosome. Following this, kinetochores associate with microtubules emanating from the two spindle poles and align at the metaphase plate in the center of the cell. Each kinetochore is attached to microtubules originating from the opposite spindle pole. When chromosomes are improperly attached to the spindle, a lack of tension is detected and the cell cycle progression is halted by the spindle assembly checkpoint (SAC) till the correct attachments are formed (Musacchio and Salmon 2007). Once metaphase is successful, anaphase is initiated by the anaphase promoting complex/cyclosome (APC/C), which degrades securin, an inhibitor of the protease, separase. Separase then cleaves the cohesins that hold the sister chromatids together, and microtubules pull the chromatids towards opposing spindle poles (Figure 1a).

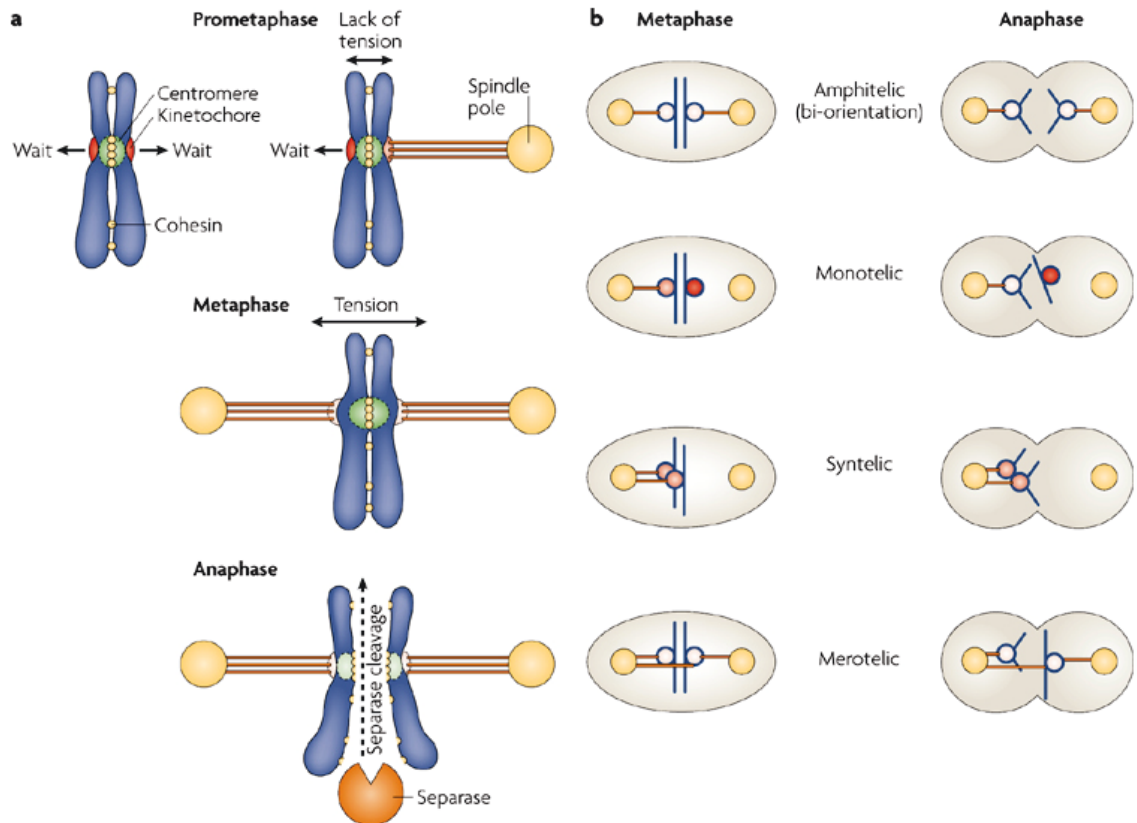


Figure 1: The attachment process during chromosome segregation (Musacchio and Salmon 2007) (a) Unattached kinetochores generate a 'wait' signal and recruit the spindle-assembly checkpoint (SAC) proteins. When sufficient tension is achieved, the SAC signal is extinguished and anaphase ensues thanks to the activation of separase, which removes sister-chromatid cohesion. (b) Correct and incorrect attachments can occur during mitosis. Monotelic attachment, or a single unattached kinetochore is a normal condition during prometaphase. The SAC might be able to sense syntelic attachment, but it is unable to detect merotelic attachment (Cimini, et al. 2001).

If the SAC is defective or the activity of separase is improperly regulated, the cell proceeds to anaphase despite incorrect microtubule attachments and this could lead to chromosome missegregation and aneuploidy (Musacchio and Salmon 2007) A premature loss of cohesins that hold sister chromatids together could also bypass the SAC and lead to random segregation of chromosomes (Nasmyth and Haering 2009). In addition, aberrant kinetochore attachments, such as when a single kinetochore attaches to microtubules emerging from both spindle poles (called merotelic attachments), could result in aneuploidy (Figure 1b) (Thompson and Compton 2011) (Musacchio and Salmon 2007). Regardless of the mechanism of generation, aneuploidy is known to have drastic effects on cell physiology.

Consequences of aneuploidy

Effects of aneuploidy on gene expression

Studies across multiple organisms suggest that the level of mRNA expression in aneuploids largely scales with gene copy number (Pavelka, et al. 2010) (Rancati, et al. 2008) (Sheltzer, et al. 2012) (Torres, Sokolsky, et al. 2007). For instance, in human tetrasomic cell lines, transcription levels across the genome were found to correlate with copy number changes and the median ratio mRNA change of ~ 2.12 was close to the expected value of 2 (Stingele, et al. 2012). However, in most studies to date, there are still genes whose expression does not mirror this gene dosage effect. Some of these genes whose expression did not correlate with copy number could be targets of transcriptional regulators which exhibit copy number alterations (Rancati, et al. 2008). Additionally, trans-acting dosage effect was observed in *Drosophila melanogaster*, where genes without copy number alterations showed altered gene expression due to a feedback mechanism which seeks to maintain gene expression homeostasis in an aneuploid genome (Stenberg, et al. 2009). Another effect is that of ‘dosage compensation’, in which genes on the extra chromosome do not scale their gene expression with copy number, but retain gene expression similar to a euploid by regulating transcription of the varied chromosome arm. In wild yeasts, some genes which are lethal when overexpressed, showed lower than expected increase when their copy number was altered (Hose, et al. 2015), it still remains to be seen whether dosage compensation plays a significant role in aneuploidy. Taken together, the effects of aneuploidy on gene expression is still under speculation, and the phenotypic consequences of aneuploidy remain elusive without common physiological signatures yet.

Phenotypes associated with aneuploidy

Aneuploidy is known to cause detrimental effects in a broad range of species from *S. cerevisiae* to humans. Haploid *S. cerevisiae* cells containing single extra chromosomes, known as disomes, display slower growth rate compared to euploid cells. In humans, aneuploidy is a common cause of several genetic disorders, and in most cases, embryonic lethality. The trisomies that survive birth, trisomy 13, 18 and 21 also known as Patau syndrome, Edward's syndrome and Down syndrome respectively, are associated with developmental delays and reduced lifespan.

Although in most cases aneuploidy negatively impacts cell growth, under certain stress conditions, aneuploidy confers a fitness advantage. For instance, in clinical isolates of the pathogenic yeast *Candida albicans*, aneuploidy bestows resistance to a common anti-fungal drug, fluconazole (Selmecki, Forche and Berman 2006). Similar observations have been made in *S. cerevisiae*, where the analyses of aneuploid strains with random chromosome stoichiometries revealed that their complex karyotypes confer an increased phenotypic variability, leading to adaptive phenotypes in multiple conditions which deviate from the ideal environment for the euploid wild type (Figure 2). In several cases, this fitness advantage was attributed to copy number changes of a subset of highly impactful genes under the specific harsh environmental conditions (Pavelka, et al. 2010).

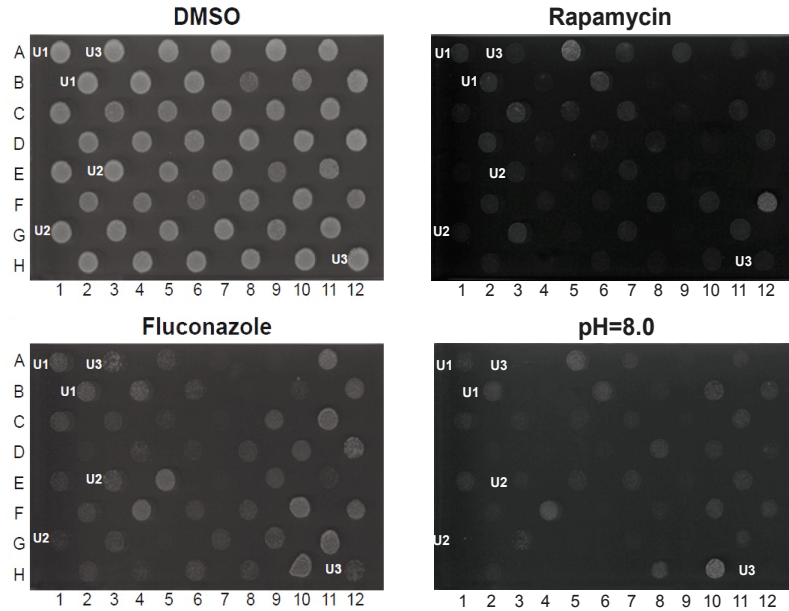


Figure 2: Aneuploidy confers phenotypic variation under diverse stresses.

Representative images of aneuploid and euploid strains on YPD plates at 23oC subject to different environmental stresses. Haploid, diploid and triploid strains are denoted by U1, U2 and U3 respectively. Compared to a DMSO control, certain aneuploid strains visibly grow better than the euploids when treated with the drugs fluconazole, rapamycin and at sub-optimal pH (Pavelka, et al. 2010)

While karyotype-specific effects of aneuploidy have been studied, little is known about possible global, karyotype-independent effects of aneuploidy. Some of the consequences of an unbalanced karyotype include a delay in the G1 phase of the cell cycle (Torres, Sokolsky, et al. 2007) and genomic instability (Sheltzer, et al. 2012). A well-studied aneuploidy-associated phenotype is proteotoxic stress. Proteotoxicity refers to a cellular state in which the protein quality control machinery of the cell is compromised, leading to

protein misfolding. Previous studies have shown that ~80% of the proteome scales with gene copy number (Pavelka, et al. 2010) (Oromendia, Dodgson and Amon 2012). This additional protein content could overwhelm the protein quality control pathway. For example, trisomies of chromosome 1, 13, 16 or 19 in mouse embryonic fibroblasts were more sensitive to 17-AAG, an inhibitor of the chaperone protein Hsp90, relative to their wild type counterparts (Tang, et al. 2011). Further, many disomic *S. cerevisiae* strains were found to be sensitive to chemical compounds that impair protein quality control (Oromendia, Dodgson and Amon 2012) (Oromendia and Amon 2014). Since these studies involved only aneuploids with alteration in copy number of a single chromosome, it still remains elusive whether proteotoxic stress is the only general stress instigated by aneuploidy, particularly in cells with random complex karyotypes.

The role of aneuploidy in cancer

A vast majority of cancers are aneuploid, which with the cancer phenotype of aggressive proliferation, is in direct contrast to the detrimental effects usually associated with aneuploidy (Mitelman, Johansson and Mertens 2006). However, the exact role of aneuploidy in tumorigenesis and cancer metastasis is unknown. One possibility is that specific cancer phenotypes could be associated with aneuploidy due to increase of oncogene copy number or decrease in the copy number of tumor suppressor genes. For instance, two of the most frequent chromosomal aberrations observed among different types of cancers were gain of chromosome 8q (encoding the *MYC* oncogene) and loss of 17p (encoding the *TP53* tumor suppressor gene) (Mitelman, Johansson and Mertens 2006) (Nicholson and Cimini 2013). Another hypothesis is that the unstable aneuploid genome

could promote tumor heterogeneity and increase the proliferative ability of cancer cells, potentiate their adaptability to chemotherapy or lead to tumor relapse (Fisher, Pusztai and Swanton 2013) (Kreso, et al. 2013) (Navin, et al. 2011). For example, Navin et al. (2011) observed subclones with distinct patterns of DNA copy number variation, derived from a common clonal progenitor, within the same sector of a primary tumor. Since cancer is characterized by cell-to-cell heterogeneity, where aneuploidy co-exists with other mutations, identification of a karyotype-independent global aneuploidy signature and an understanding of the molecular mechanisms governing this commonality could help design effective therapeutic strategies to target cancer.

***Saccharomyces cerevisiae* as a model system to study aneuploidy**

Budding yeast *S. cerevisiae* is an extensively studied unicellular eukaryote with a small genome composed of sixteen chromosomes and few intergenic regions (~ 30% of the genome). Further, the yeast genome is well annotated, and majority of genetic pathways are conserved in more complex eukaryotes. Budding yeast is often used as a model system to study aneuploidy since it is relatively tolerant of aneuploidy (reviewed in (Mulla, Zhu and Li 2013)), and powerful yeast genetics enable the generation of isogenic aneuploid strains without other changes to the genome. One method exploits the random segregation of homologous chromosomes during meiosis I in a yeast strain with an odd ploidy. During meiosis I, a parental diploid yeast cell undergoes equal segregation of its sister chromatids to give rise to four haploid progenies with uniform karyotype. However, in case of a triploid strain, the meiotic process gives rise to aneuploid progenies with random karyotypes (Figure 3). This collection of aneuploid strains with random chromosome stoichiometries

mimics the karyotypic complexity associated with cancer cells exhibiting high occurrence of chromosome instability.

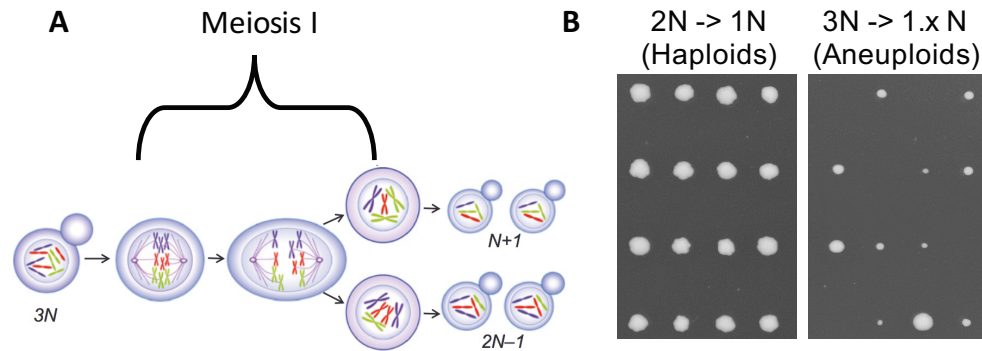


Figure 3: Triploid meiosis gives rise to aneuploid progenies. (A) Illustration of triploid meiosis (Mulla, Zhu and Li 2013). (B) Spores from dissection of diploid and triploid tetrads. Each row of representative spores is from a single tetrad (adapted from Hung-Ji Tsai [unpublished data])

Aim of Research

Aneuploidy has profound and divergent effects on cell physiology. This thesis was centered on identifying features that were inherent to the aneuploid state, irrespective of karyotype, utilizing the model system of budding yeast *Saccharomyces cerevisiae*. Firstly, we aimed to uncover a potential aneuploidy-associated gene expression profile which was not confounded by transcriptome changes that were specific to chromosome stoichiometries. The karyotype specific transcriptional response was ruled out by exploiting random meiotic segregation in triploid yeast to generate karyotypically heterogeneous aneuploid populations. These populations were sufficiently large for the population average of

chromosome copy number for every chromosome to be equal, as predicted by a general statistical model. Thus, a gene expression profile consistent across all aneuploid strains would stand out. Another specific aim was to determine whether the transcriptional signature in aneuploid cells would manifest as phenotypes characteristic of the transcription program observed. Taken together, the fulfillment of these research aims would have interesting insights from both the basic biology perspective of understanding the molecular mechanisms of aneuploidy as well as in the context of diseases such as cancer. In cancer, the ability of karyotypic heterogeneity to potentiate adaptability to existing drugs is a major obstacle to effective cancer therapeutics (Kreso, et al. 2013) (Fisher, Puztai and Swanton 2013). If aneuploid cells, regardless of karyotypic complexity, exhibit a common signature or a predilection for particular genetic pathways, targeting this global feature of aneuploidy could pave the way for novel therapeutics.

Materials and Methods

Yeast strains and growth condition

Aneuploid and euploid strains were generated by the method of yeast meiosis (Pavelka et al. 2010). Diploid and triploid strains originated from BY4741 background were sporulated in SPM media in 23 °C for four to five days, and tetrads were dissected on YEPD plates to grow in 23 °C for five days. In addition, a high-throughput method to generate aneuploid strains with random karyotypes was developed by following a modified protocol of synthetic genetic array analysis (SGA) (Tong et al. 2006, and Hung-Ji Tsai, unpublished method). Briefly, meiotic progenies from diploid or triploid parental strains carrying a plasmid (pRS315) with a auxotrophic marker (*spHIS5*) fused with a mating-type specific promoter (*STE2pr*) were selectively grown on SC-His-Leu plates (a modified medium recipe from Tong et al 2006) in 23 °C for five days. For the follow experiments (described later), euploid or aneuploid colonies were grown in YEPD media overnight (16 hours) at 25 °C.

In the DNA-seq and RNA-seq experiments, 960 aneuploid strains from tetrad dissection and 2880 aneuploid strains from auxotrophic selection were grown overnight and then 300 µl fresh YEPD media were added for another four hours of growth before being pooled into individual groups. At the end, five groups as biological replicates were gathered with 960 aneuploid strains in each group for further sequencing analysis. For the microscopy or other experiments (described in later session), at least 180 aneuploid strains were normalized into the same cell number based on the optical density (OD) from the overnight culture before pooled as a heterogeneous aneuploid population. Both haploid strains and aneuploid population were diluted to OD ~0.3 and grown in SC or YEPD rich media at 30

°C for 2-4 hours. The experimental procedures were performed with help from Hung-Ji Tsai.

Statistical model for determination of aneuploid population size

Model assumptions

The karyotypic state of individual strains of the aneuploid population were assumed to be independent of each other. In addition, within a strain, copy number change of one chromosome is not presumed to influence copy number variation in other chromosomes. Copy number states within a strain are restricted to either 1 or 2.

Mathematical design

Each strain follows a random binomial distribution with either 1 or 2 copies of individual chromosomes.

$$Y \sim B(n = 16, p) \quad \frac{1}{16} \leq p \leq 1$$

where, $n = 16$ is the number of chromosomes and probability p of copy number alteration is a random variate.

Relative chromosome copy number (RCC) in a strain k was defined as ratio of the copy number of chromosome I in the strain to the average copy number of the other chromosomes in the same strain.

$$F_k = \frac{15Y_{(k,1)}}{\sum_{m=2}^{16} Y_{(k,m)}}$$

where $Y_{(k,m)}$ is the copy number of chromosome m in strain k .

Mean and standard deviation (SD) of RCC as a function of population size s were calculated as follows:

$$\bar{F}_s = \frac{\sum_{k=1}^s F_k}{s}$$

$$\sigma_s = \sqrt{\frac{\sum_{k=1}^s (F_k - \bar{F}_s)^2}{s}}$$

The population size below which the absolute value of the first order derivative of the 95% confidence interval (CI) for RCC mean as well as SD was below 10^{-5} , was estimated as a reasonable minimum population size $s_{critical}$.

$$s_{critical} = \arg \min_s \left(\left| \frac{\partial(CI(\bar{F}_s))}{\partial s} \right| - 10^{-5} \right)$$

To confirm an approximate range for the population size, multiple iterations of the entire workflow were performed. The entire pipeline was implemented in R (v. 3.3.2)

Next Generation Sequencing (NGS) data analysis pipeline

Data pre-processing and quality control

Raw reads sequenced by Illumina MiSeq were checked for read quality using FastQC (v. 0.11.5). Per base sequence quality (phred > 20) and GC content were consistent across all samples for both DNA and RNA-seq.

Copy number analysis

The whole genome sequence of *Saccharomyces cerevisiae* strain S288c (Release no. R64-2-1) was obtained from the Saccharomyces Genome Database (SGD). Single-end reads (~150bp) were mapped to the reference genome using the alignment tool Bowtie 2 (Langmead and Salzberg 2012) and uniquely mapped reads were extracted using SAMtools (Li, et al. 2009). To estimate the copy number, reads binned by variable bin width between 500bp to 2000bp were median normalized to make counts comparable across samples. Normalized aneuploid population profiles were then referenced to an associated euploid population control profile and the ratio was log₂ transformed. An R script using the circular binary segmentation algorithm implemented in the Bioconductor package DNACopy (v. 1.48.0), was used to identify genomic regions with copy number alterations utilizing a haploid strain as the reference.

Transcriptome analysis

Single-end reads from stranded RNA sequencing were mapped to the annotated *S. cerevisiae* reference genome S288c (Release no. R64-2-1) using the HISAT2 aligner (Kim, Langmead and Salzberg 2015). SAMtools was used to sort, index and convert the .sam file to the required .bam format. Raw counts per gene were generated using HTSeq (Anders, Pyl and Huber 2015). Differentially expressed genes in the aneuploid populations relative to euploid populations were identified using the Bioconductor package DESeq2 (Love, Huber and Anders 2014). Prior to analysis, genes with average read count less than 5 were filtered out. Data quality was assessed by principal component analysis (PCA) and distance

based sample clustering. To rule out effects specific to the method of generation of aneuploid populations, a factor accounting for the different methods was incorporated into the model design. The contrast factor was solely based on whether a population was euploid or aneuploid. In other words, this model checked for aneuploidy specific change in gene expression consistent across all aneuploid populations.

The Benjamini-Hochberg (BH) corrected p-value was calculated on the Wald statistic to account for multiple hypothesis testing. Since our data exhibited an enrichment of low p-values, to control for false positives, the obtained result was further corrected for variance underestimation by applying empirical null modeling. The R package `fdrtool` (v. 1.2.15) was used to calculate the false discovery rate (FDR) based on empirical variance of the null distribution. Differentially expressed genes (DGE) were defined as genes with a FDR less than 5%. DGE were inspected for GC content, chromosomal location and gene length bias.

Comparison of transcriptome results to published datasets

Aneuploid population transcriptome was compared to the genomic expression response of *S. cerevisiae* to various environmental stresses published by Gasch et al (2000). The spearman rank correlation coefficient between our dataset and individual stresses from Gasch et al. were calculated using pairwise complete, fold change observations, which covered upwards of 90% of the whole genome. In addition to a whole genome network, a correlation network was constructed using only the differentially expressed genes in the aneuploid population.

The correlation network was constructed using a custom R script, implemented with the CRAN package `ggnetwork` (v. 0.5.1). The vertex positions in the network are based on the

eigenvectors and eigenvalues of the whole genome expression correlation matrix of the genomic profiles in Gasch et al.

Comparison to RNASeq data of Cromie et al. (2016) was performed by running our NGS pipeline (described above) on the samples versus counts matrix deposited by the authors in the GEO database (Langmead and Salzberg 2012), followed by a Spearman rank correlation test.

Monitoring cell swelling

Aneuploid and haploid populations were freshly prepared as described earlier for the following experiments. For the microscopy analysis, cells were immobilized on a glass-bottomed 96-well plate. Plates were coated with 100 μ l of 1mg/ml Concanavalin A and placed in a desiccator for 4- 6h. Wells were washed once with 200 μ l of water followed by 200 μ l of SC media and dried in a desiccator for 4h. 200 μ l of cell culture was plated per well. Plates were sealed and spun at 300 g for 2 min. Cells were imaged over 17 hours on a Nikon Ti Eclipse microscope. All images were collected with a Nikon Plan Apo 40x air objective using Nikon NIS Elements software to drive stage movement and acquisition. Cell size analysis was performed on the Nikon NIS Elements AR software.

Measurement of glycerol concentrations

Intracellular and extracellular glycerol were measured enzymatically using a commercial glycerol assay kit (Sigma Aldrich). Aneuploid populations were freshly prepared as described earlier and cell populations were collected in different time point after the pooling step. Cells were pelleted by centrifugation, and the supernatant was collected for

measurement of extracellular glycerol. For the measurement of intracellular glycerol, cell pellets were then washed with 2 ml ice-cold YEPD, and resuspended in 1 ml 0.5 M Tris-HCl, pH 7.5, by vortexing. Samples were heated to 95°C for 10 min, and cell debris was removed by centrifugation. Glycerol determinations were performed as per manufacturer's specifications.

Intracellular viscosity assay

Aneuploid and haploid populations were prepared freshly as described earlier. Cells were incubated with DCVJ (Ursa Bioscience) as per manufacturer's specifications for 30 minutes. To reduce background and prevent further passive diffusion of the dye, cells were washed twice with media prior to imaging. DCVJ fluorescence intensity data was collected with a FITC filter and Nikon Plan Fluor 100x objective. A semi-automated image analysis pipeline implemented in Nikon NIS Elements AR software involving rolling ball background correction, thresholding and segmentation was used to determine total fluorescence intensity and size per cell.

Endocytosis assays

Aneuploid and haploid populations were prepared freshly as described earlier. FM4-64 recycling was assessed as described elsewhere (Lang, et al. 2014). Briefly, cells grown to log-phase were immobilized in a homemade chamber on a microscopic slide, coated with 1mg/ml Concanavalin A for 30 minutes. Appropriate media supplemented with 0.46µg/ml FM4-64 was added to the chamber at 4°C. After 15 min, cells were washed three times in ice-cold media and kept on ice till imaged. For sorbitol rescue experiments, 1 M sorbitol was added just prior to imaging. FM4-64 dynamics were captured every minute using the

mCherry filter and Nikon Plan Apo 40x air objective with magnification increased to 1.5x on a Nikon Ti Eclipse epifluorescence microscope. Background correction was applied to every frame and the endocytosis readout was the ratio of mean intensity of FM4-64 intensity in the cytoplasm to the mean intensity at the plasma membrane.

To measure Abp1p dynamics, Micrographs of GFP-tagged Abp1p in euploid and aneuploid populations were captured every second for up to 60 seconds using a FITC filter and Nikon Plan Fluor 60x objective. Kymographs of Abp1 patches were created and analyzed using ImageJ.

Zymolyase sensitivity assay

Aneuploid strains were grown overnight in individual wells of a 96-well deep well plates in 200 μ l of YEPD. Cultures were then refreshed in 200 μ l of YEPD for 2 hours and pooled together after normalization to OD₆₀₀ of 0.5. Cultures were transferred to wells of a 96-well plate and 100 μ l of 50 μ g/ml of zymolyase was added. OD₆₀₀ was measured every 15 minutes up to 90 minutes.

Statistical Analysis

Statistical significance for increased glycerol efflux in the aneuploid population as well as decrease in intracellular glycerol was determined using a one-tailed t-test. Difference in bulk intracellular viscosity between euploid and aneuploid populations was determined by a one tailed t-test for the alternate hypothesis that aneuploid populations had a lower viscosity.

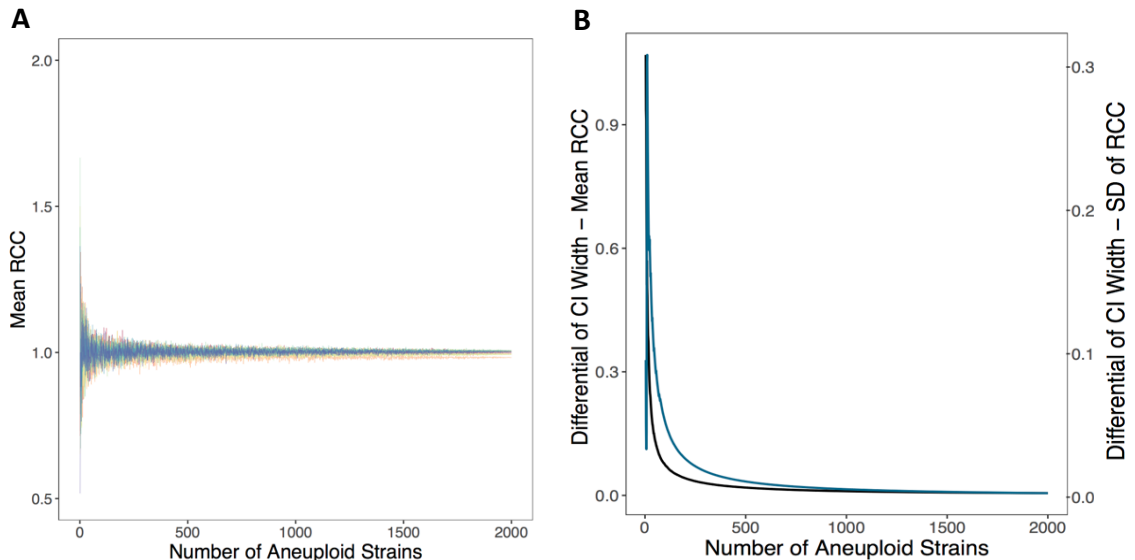
Results

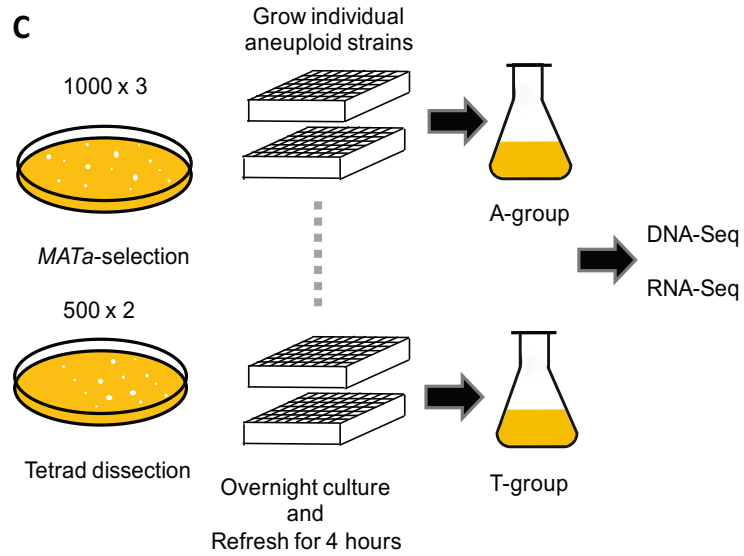
Generation of aneuploid populations with uniform ploidy distribution

Gene expression in aneuploidy generally scales proportionally with the gene copy number and varies across aneuploid cells bearing different karyotypes. Thus, common transcriptional signatures in aneuploidy, if any, could be masked by the karyotype specific transcriptional response. Alternatively, in the overall transcriptional response in a karyotypically heterogeneous population, the karyotypic specific features could be minimized presumably due to the equal frequency of appearance of each aneuploid chromosome in a karyotypically diverse aneuploid population, provided the population size is large enough. On the other hand, if there is a common transcriptional signature across the population, the expression of genes associated with this global response would stand out. Thus, to investigate whether aneuploids, regardless of karyotype, exhibited consistencies in gene expression, we generated a heterogeneous aneuploid population with the apparent ploidy distribution similar to a euploid karyotype. The size of the heterogeneous aneuploid population required was determined by a general mathematical model (see Methods) which determines the population size at which the ratio of copy number of a chromosome in a population to the average copy number of the remaining chromosomes – a quantity we term as relative chromosome copy number (RCC), converges. The minimum required population size beyond which the average and standard deviation of the RCC remain nearly constant, implying an equal appearance of each aneuploid chromosome, was estimated to be less than 400 aneuploid strains (Figure 4A and 4B). The model was validated by genome Illumina sequencing performed on the aneuploid populations derived by two independent methods, tetrad dissection and mating

type specific auxotrophic selection (Figure 4C, also described in Methods) (Tong and Boone 2006), and compared to euploid populations, which were generated by the same method, as well as a haploid control. Analysis of the DNA-seq data revealed that genome content of aneuploid populations was similar to euploid populations as predicted by the model (Figure 5 , Table 1.1). From copy number analysis implementing the circular binary segmentation algorithm, no gene showed consistent change in copy number across all aneuploid populations sequenced. (Table 1.2)

Figure 4: Model estimation of aneuploid population ploidy distribution. (A) Mean of the relative chromosome copy number (RCC) for each of 16 chromosomes. (B) Rate of convergence of the confidence interval for mean RCC (*black*) and SD of RCC (*blue*). (C) Illustration of the two methods of deriving aneuploid populations.





Chromosome	Copy Number				
	Taneu1	Taneu2	Aaneu1	Aaneu2	Aaneu3
I	0.89	0.95	1.07	1.10	0.81
II	1.07	1.12	0.96	0.99	0.99
III	1.09	1.08	0.86	0.86	0.86
IV	1.08	1.10	1.15	1.19	1.16
IX	1.10	1.05	1.03	1.06	1.07
V	1.05	1.05	0.92	0.91	0.90
VI	0.84	0.86	0.84	0.85	0.82
VII	1.01	1.05	1.00	1.01	0.99
VIII	0.92	0.98	1.12	1.12	1.12
X	0.94	1.01	0.93	0.95	0.93
XI	1.11	1.03	1.06	1.14	1.13
XII	1.05	1.11	1.02	1.03	1.01
XIII	1.11	1.17	1.10	1.11	1.10
XIV	1.00	0.99	0.92	0.95	0.93
XV	0.89	0.91	0.96	0.98	0.98
XVI	1.08	1.10	1.08	1.16	1.13

Table 1.1 Mean chromosome copy number of aneuploid populations. Taneu: populations derived by tetrad dissection Aaneu: populations derived by mating type specific auxotrophic selection. Copy number is measured relative to euploid populations.

Chromosome	Gene	Populations with CNV	Copy Number
I	FLO1	Taneu1	2
I	ARS112	Aeu	2
II	LYS2	All except Aeu	0
IV	TMA64	Taneu1	2
IV	ZIP1	Aaneu2	2
VI	COS4	Taneu1	2
VIII	YHR214C-C	Taneu1	2
IX	TEL09R	Taneu1	2
XII	ARS1200-1	All populations	2
XIV	TEL12R	Aaneu2	0

Table 1.2 Copy number variants in euploid or aneuploid populations. Results of copy number variant analysis with haploid control as reference. Table indicates variants and which populations possessed this copy number alteration.

Population transcriptomics reveal a global aneuploidy gene expression signature

Strand-specific RNA-Seq was performed on RNA extracted from the same populations used in DNaseq experiments, comprising of ~4000 individual aneuploid strains with random chromosome stoichiometry. To assess the variation across all biological samples, both aneuploid and euploid populations, principal component analysis (PCA) as well as sample distance approximation were performed. As expected, a significant proportion of the variance reflected the difference between euploid and aneuploid populations. Additionally, aneuploid populations generated by the two methods, with and without auxotrophic selection, showed a minor difference as indicated by the PCA (Figure 6A).



Figure 5: Aneuploid populations display uniform ploidy. Results of whole genome sequencing for aneuploid and euploid populations relative to a haploid control. Mean for each chromosome (*red dashed lines*) was close to 1 across all chromosomes .

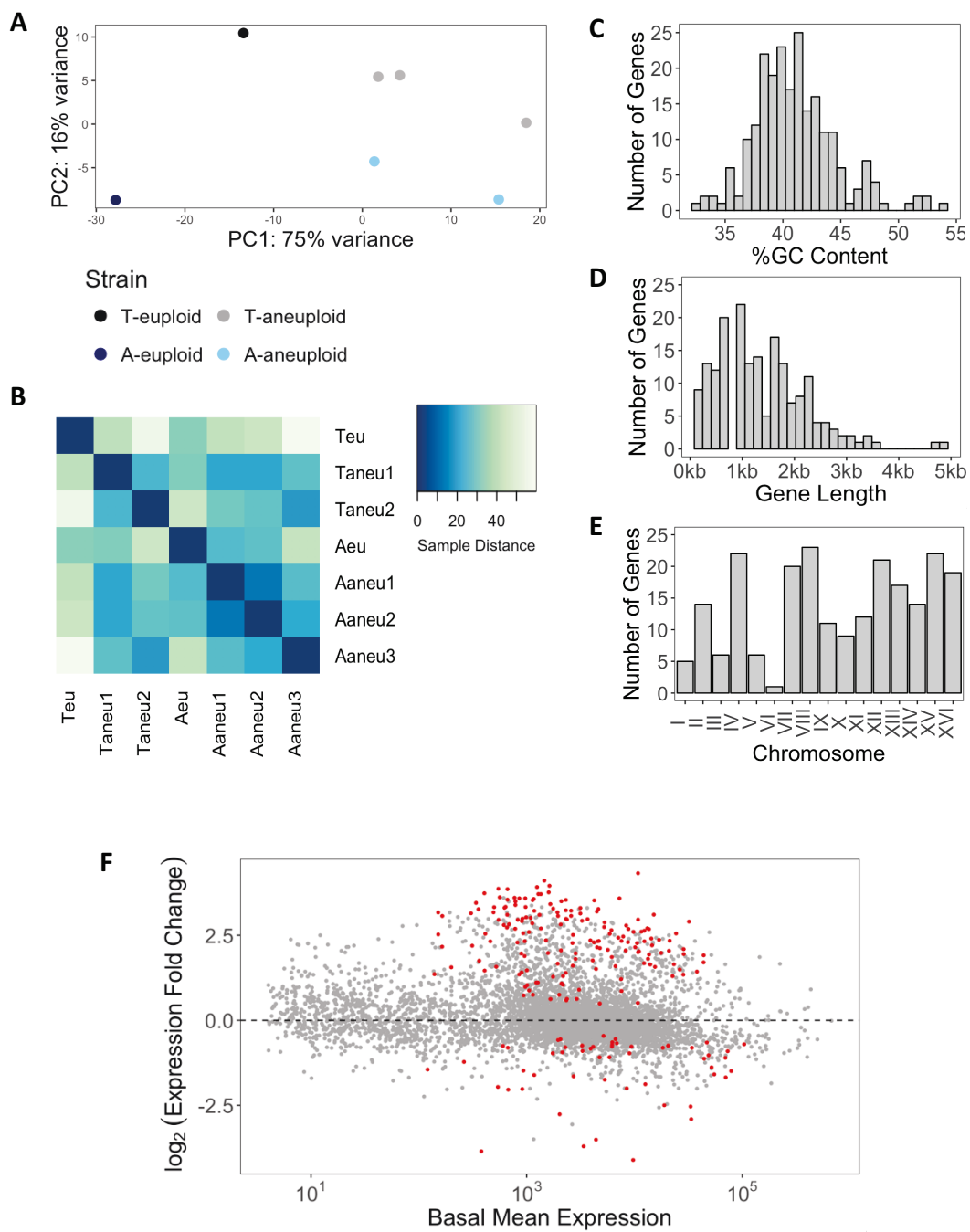


Figure 6: Transcriptome analysis of aneuploid populations. (A) Principal component analysis of RNAseq counts. PC2 appears to reflect a small difference in the two methods of generation of aneuploid populations. (B) Sample distance matrix indicating difference

between samples. The GC content (C), gene length (D) and chromosomal location of differentially expressed genes reveal no biases. (F) MA plot of aneuploid populations relative to euploid populations. Significant genes are marked in red.

In order to identify the transcriptional response specifically due to aneuploidy without the influence of the method used to generate the aneuploid populations, a factor controlling for this effect was incorporated into the statistical analysis (see Methods), which revealed 222 significant differentially expressed genes (FDR < 5%) across all the aneuploid populations relative to the euploid populations (Figure 6F). The differentially expressed genes showed no bias with respect to GC content, gene length or chromosomal location (Figure 6 D, E, F).

Identification of an aneuploidy driven stress response

Aneuploid population transcriptome resembles transcriptional signatures of cells under hypo-osmotic shock and cell wall stress.

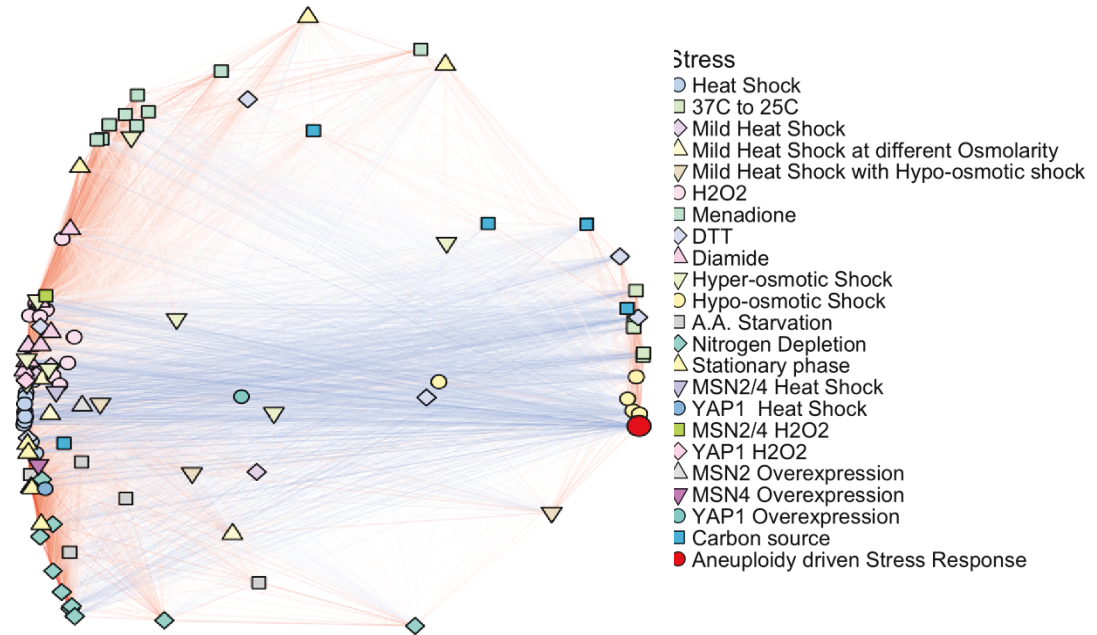
The gene expression profile of the aneuploid population was compared to gene expression patterns of the response of *Saccharomyces cerevisiae* to 141 diverse environmental transitions reported by Gasch et. al. (2000) (Figure 7A). Interestingly, the aneuploid transcriptome signature was positively correlated (Figure 7E) with less than 10% of the tested conditions, implying that the aneuploidy stress is highly specific. The highest correlation was observed with hypo-osmotic shock (Figure 7B) and short-term treatment with the reducing agent, dithiotheritol (DTT) (Figure 7C). While long-term DTT exposure

disrupts ER function and causes an accumulation of misfolded or unfolded proteins in the ER lumen (Jamsa, Simonen and Makarow 1994), initial exposure directly affects the disulfide bonds of the cell wall (Gasch, et al. 2000). This suggests that aneuploidy-specific stress might be similar to cell wall stresses.

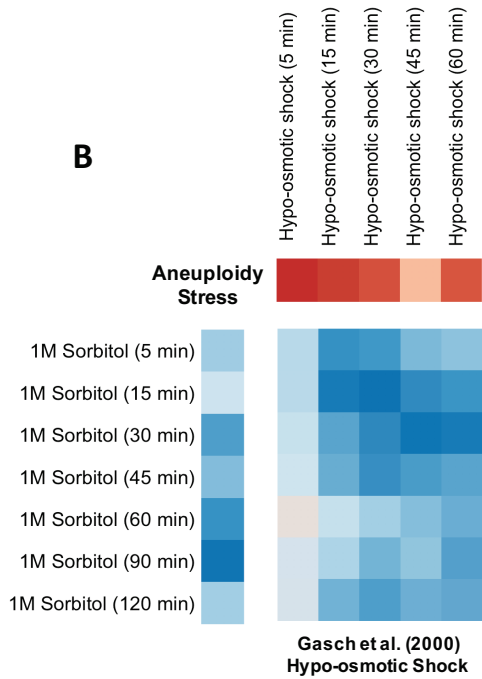
Aneuploidy stress does not correlate with ESR induction.

The ESR refers to a transcriptional response induced in yeast cells response to abrupt detrimental environmental changes, including heat shock, hyper-osmotic shock, amino acid starvation and redox stresses. Some characteristic features of the ESR are the transcriptional repression of genes involved in growth processes such as ribosomal biogenesis and translation initiation, and the induction of genes related to DNA damage repair, protein quality control, autophagy etc. (Gasch, et al. 2000). Previous studies have reported that disomic aneuploid budding yeast cells exhibit a transcription signature similar to the ESR (Sheltzer, et al. 2012) (Torres, Sokolsky, et al. 2007). Strikingly, we observed that the aneuploid transcriptome was strongly anti-correlated (Figure 7A, 7E) with DNA microarray expression results from Gasch et al. for environmental conditions associated with ESR induction including heat shock and prolonged DTT exposure (Figure 7C). In a recent study, Cromie et al. (2015) pooled together 3-5 colonies from two disomic aneuploid budding yeast strains (Disome XV and Disome XVI) generated by auxotrophic, mating-type specific selection in the F45 strain background after four days of growth and performed transcriptome analyses on the pooled strains. In both disomes, they reported a transcriptional signature of ESR repression relative to a haploid pool, which is in agreement with our observations (Figure 7D).

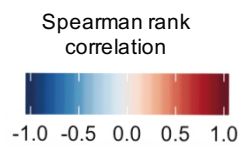
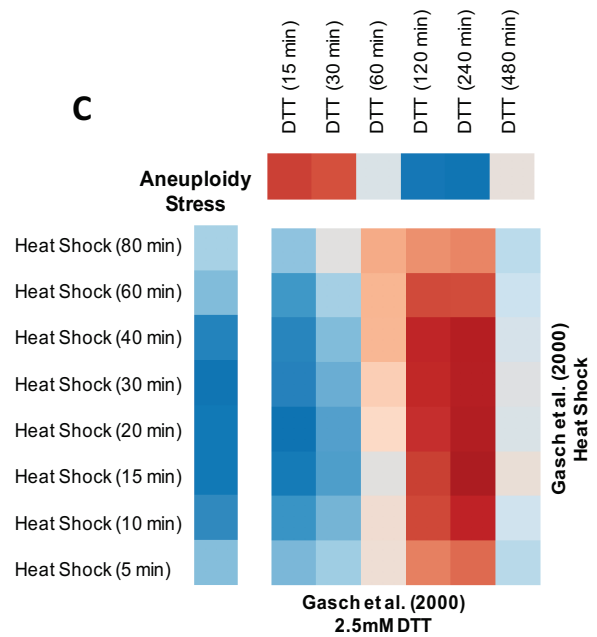
A

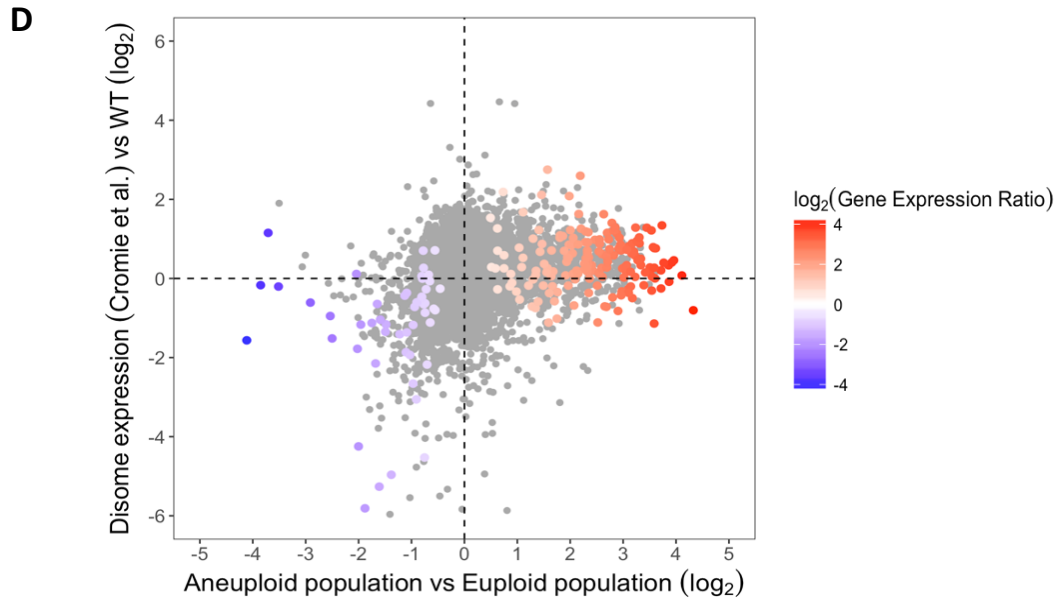


B



C





E

Stress from Gasch et al.	Spearman Rank Correlation	
	222 Significant Genes	Whole Genome
Hypo-osmotic shock (15 min)	0.717539685	0.44051726
37C to 25C (15 min)	0.697695934	0.418161482
2.5mM DTT (15 min)	0.602129171	0.415061908
Carbon source: Sucrose	0.509267548	0.353266847
2.5mM DTT (120 min)	-0.735986437	-0.412917263
1M. sorbitol (15 min)	-0.744607806	-0.513916
Heat Shock (15 min)	-0.754192346	-0.606176427
Nitrogen Depletion (30 min)	-0.767435436	-0.462040981
1.5 mM Diamide (30 min)	-0.775497882	-0.528044804

Figure 7. Comparison of the aneuploidy transcriptome to published gene expression profiles. (A) Correlation network between aneuploidy stress and stresses from Gasch et al. (2000). Strength of the spearman rank correlation is represented by distance between the stresses and edges linking them from positive (*red*) to negative (*blue*) correlation.

(B, C) Spearman rank correlation between aneuploid population transcriptome and results from Gasch et al. (2000) reveals a positive correlation to hypo-osmotic shock (B) and a positive correlation with DTT treatment (C) at 15 and 30 minutes. (D) Comparison of RNAseq data from disome XV of Cromie et al. to the aneuploid population results. 222 significant genes in our dataset are color coded by fold change. (E) Representative correlations between either whole transcriptome of the aneuploid population or differentially expressed genes in the population with microarrays from Gasch et al. (2000).

Phenotypic consequences of the aneuploidy stress response

Aneuploid cells exhibit excessive cell swelling

When *S. cerevisiae* is subject to an osmotic downshift or hypo-osmotic shock, the altered osmotic gradient leads to sudden influx of water, causing the cell to swell and resulting in an increase in turgor pressure (Hohmann 2002) (Klipp, et al. 2005). The cell wall counterbalances this turgid force by modulating its rigidity and prevents bursting of the cell (reviewed in (Levin 2005)).

To examine whether aneuploidy stress has similar morphological consequences to hypo-osmotic stress, aneuploid and euploid strains were grown under culture conditions used for the transcriptome analysis, and ~300 individual cells were monitored in parallel by time-lapse brightfield microscopy. Several aneuploid cells were much larger than the euploid cells, with a diameter almost four-fold that of the euploids (Figure 8). Over the course of imaging, some of these large aneuploid cells appeared to have burst (Figure 8B, right), implying a possible failure of the cell wall to confine cell swelling.

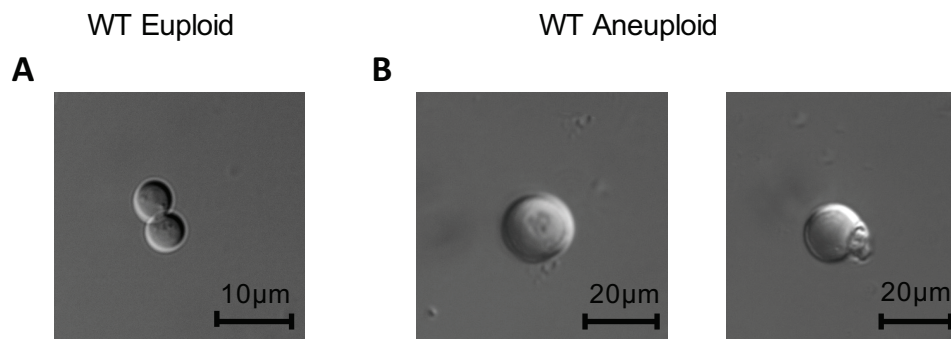


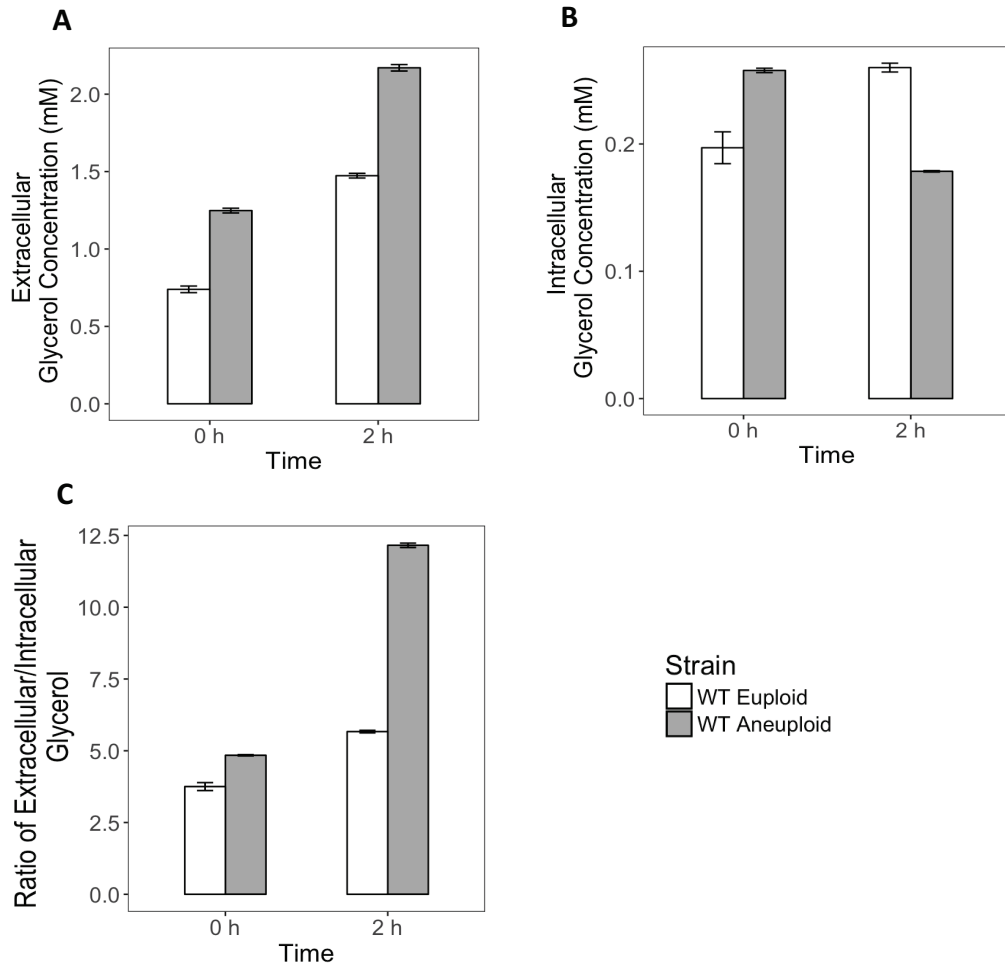
Figure 8: Aneuploid cells exhibit hypo-osmotic cell swelling. Representative micrographs of euploid (A) and aneuploid cells (B). Diameter of aneuploid cells were approximately four-fold of the euploid cells. Some of the cells appeared to have burst (*right*).

Glycerol efflux is increased in aneuploid strains

S. cerevisiae, upon hypo-osmotic shock, rapidly excretes glycerol, as an osmolyte, by both active transport and passive diffusion, to control its turgor pressure (Hohmann 2002) (Klipp, et al. 2005). Since we observed a transcriptional signature similar to hypo-osmotic stress (Figure 7B) as well as a corresponding phenotype of cell swelling in aneuploid cells (Figure 8), we examined whether aneuploid cells also displayed an increased efflux of glycerol. The concentration of extracellular and intracellular glycerol was enzymatically assayed in both euploid and aneuploid populations at 0 hours and 2 hours after pooling the populations (see Methods). As determined by a one-tailed t-test, aneuploid cells exhibited significantly ($p < 0.0001$) higher extracellular glycerol concentrations at both time points (Figure 9A). Intracellular glycerol concentration of the aneuploid population significantly decreased ($p < 0.0001$), after 2 hours in culture (Figure 9B), the result of which was a

dramatic increase in the ratio of intracellular to extracellular glycerol concentrations (Figure 9C). This increase in efflux of glycerol is characteristic of the yeast cell response to an osmotic downshift.

Figure 9: Extracellular and intracellular glycerol concentrations are altered in aneuploid cells. Extracellular glycerol (A) and intracellular glycerol concentration (B) in euploid and aneuploid populations at time 0 and 2 hours after strains were pooled. (C) Ratio of extracellular to intracellular glycerol concentrations is significantly higher in aneuploid populations after 2 hours. Error bars denote the standard error of replicates.



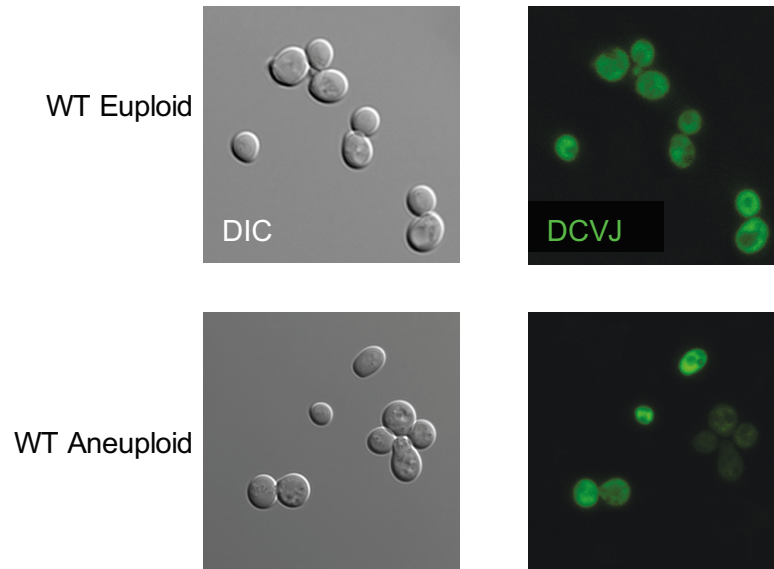
Aneuploid cells possess lower bulk intracellular viscosity

Osmotic flux is a major regulator of molecular crowding. The degree of molecular crowding within a cell is known to play a role in several cellular processes including structural modification of the cytoplasm, cytoplasmic viscosity as well as the rate of biochemical reactions (Mourao, Hakim and Schnell 2014). Miermont et al. (2013) observed that when yeast cells are subject to hyper osmotic stress, the rate of the nuclear translocation of several proteins scales proportionally with the volume fraction, and inversely with the cytoplasmic viscosity. To determine whether aneuploidy stress is associated with a change in viscosity, we measured the bulk intracellular viscosity by 9-(2,2-Dicyanovinyl)julolidine (DCVJ), a viscosity dependent fluorescent probe. DCVJ is part of a class of compounds called molecular rotors, whose fluorescence intensity and fluorescence lifetime are a function of intramolecular rotation, which varies inversely with the viscosity of the probe microenvironment (Haidekker and Theodore 2007) (Kuimova, et al. 2008). Analysis of fluorescence intensity from images captured by an epifluorescent microscope revealed that 79% of aneuploid cells ($n = 200$) had a lower viscosity ($p < 10^{-16}$) relative to euploid cells which were imaged in parallel. However, there was clearly a sub-population of aneuploid cells that possessed a viscosity comparable to the euploid population. (Figure 10 B). This is potentially reflective of recovery of this subset of aneuploid cells from hypo-osmotic stress and implies that the hypo-osmotic stress is adaptable.

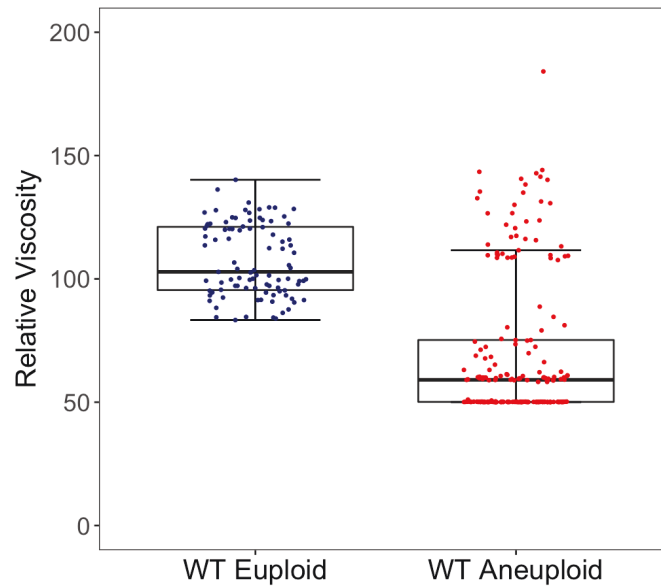
Figure 10: Bulk intracellular viscosity is shifted in aneuploid populations. (A) Representative micrographs of euploid and aneuploid cells incubated with DCVJ.

Aneuploid cells display a heterogeneity in fluorescence intensities. (B) Relative viscosity of euploid (blue) and aneuploid (red) cells. An outlier population (above upper whisker) of aneuploid cells with viscosity similar to euploids is observed.

A



B



Aneuploid cells display increased sensitivity to zymolyase

The cell wall affords yeast cells the structural support required to oppose turgor pressure (Hohmann 2002). Our observation of aneuploid cells bursting on cell swelling (Figure 8B, right) suggests that the cell wall is unable to counteract the turgor pressure and might be compromised. Integrity of the cell wall can be assessed by the susceptibility of yeast cells to zymolyase, an enzyme that degrades β -1,3-glucan network in the cell wall and leads to the activation of the transcriptional response to cell wall stress (Garcia, et al. 2009) Existing cell wall stress can cause an increased sensitivity to zymolyase and lead to cell lysis. This can be measured as a decrease in the optical density of the culture (OD_{660}). On treatment with zymolyase, aneuploid cells displayed an increased sensitivity relative to euploid cells, indicating that the cell wall was compromised in aneuploid cells (Figure 11).

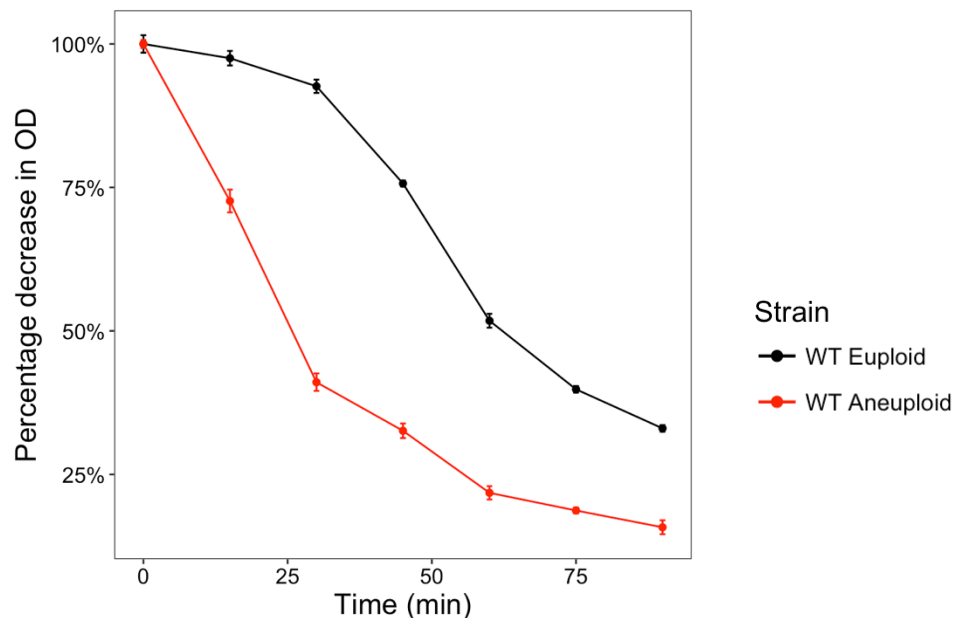


Figure 11: Aneuploidy enhances zymolyase sensitivity. Aneuploid cells (*red*) display decreased resistance to a zymolyase compared to a euploid population (*black*) as indicated

by the decrease in OD₆₆₀ after addition of 50µg/ml of zymolyase. Error bars denote the standard error.

Endocytosis is reduced in aneuploid cells

Optimal turgor is critical for the maintenance of cellular homeostasis. In budding yeast, changes in turgor pressure regulate cell wall synthesis (Piao, Machado and Payne 2007), osmotic response (Hohmann 2002) and mechanics of the plasma membrane (Basu, Munteanu and Chang 2014) (Proctor, et al. 2012), including endocytosis. Endocytosis is a process involving the local ingression of the plasma membrane that eventually forms an endocytic vesicle. Turgor pressure opposes membrane deformation during invagination of the endocytotic pit, and increases the amount of force that has to be generated by the endocytic machinery. For instance, in fission yeast, *Schizosaccharomyces pombe*, decreasing effective turgor pressure by addition of sorbitol to growth media significantly accelerated early steps in the endocytic process (Basu, Munteanu and Chang 2014) . Endocytosis is important for maintenance of membrane homeostasis, modulation of signal transduction and nutrient uptake (McMahon and Boucrou 2011). Defects in endocytosis have been linked to reduced growth in budding yeast (Grote, et al. 2000) and tumorigenesis (Joffre, et al. 2011).

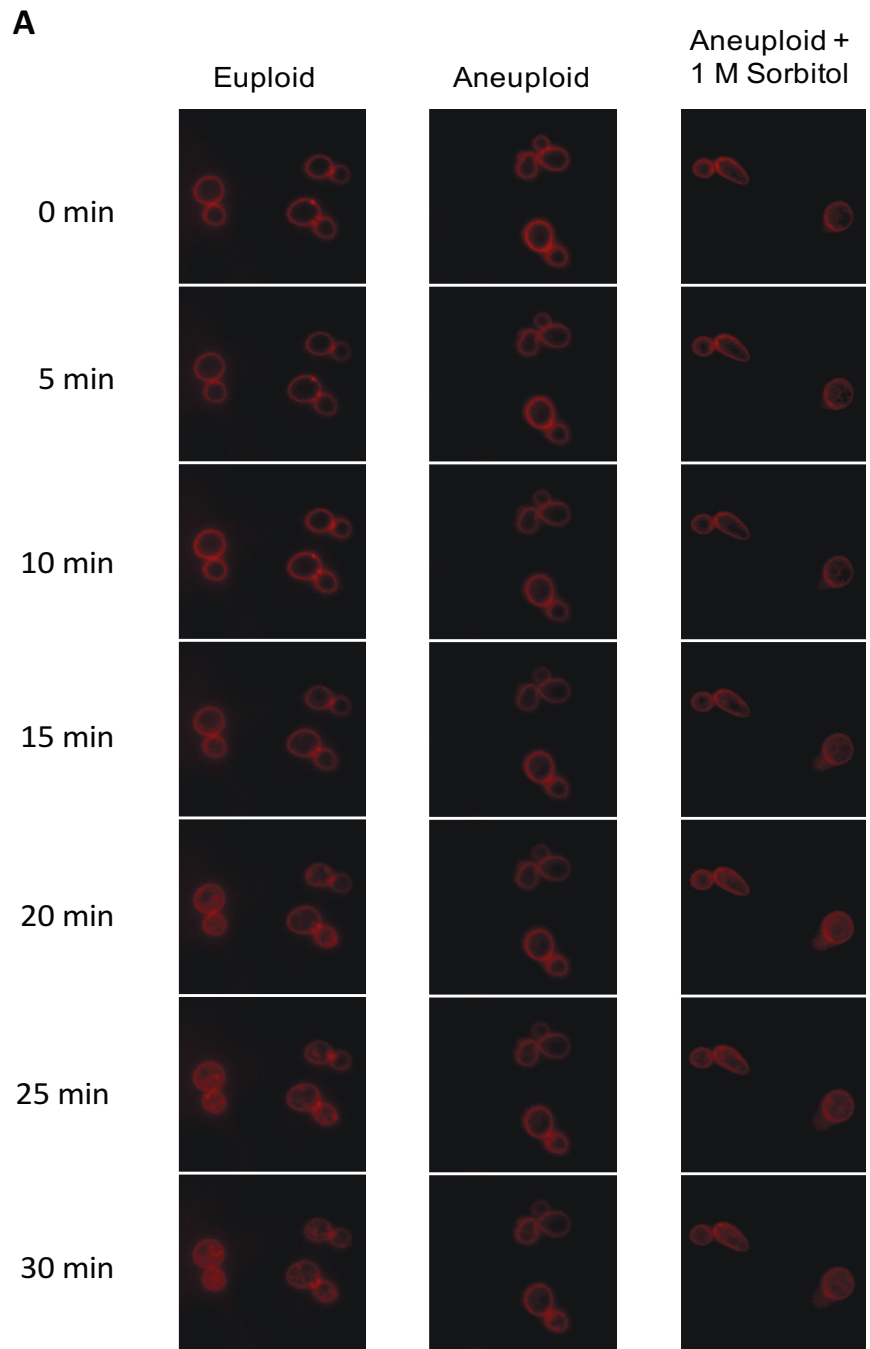
To determine whether endocytosis was compromised in aneuploid cells, we analyzed bulk plasma membrane turnover using a fluorescent lipophilic probe, FM4-64. FM4-64 internalization was measured at the resolution of 1 minute for up to 30 minutes. Endocytosis was visibly delayed in aneuploid cells. (Figure 12 A, B). It is possible that the increased turgor pressure could increase plasma membrane tension and counteract the

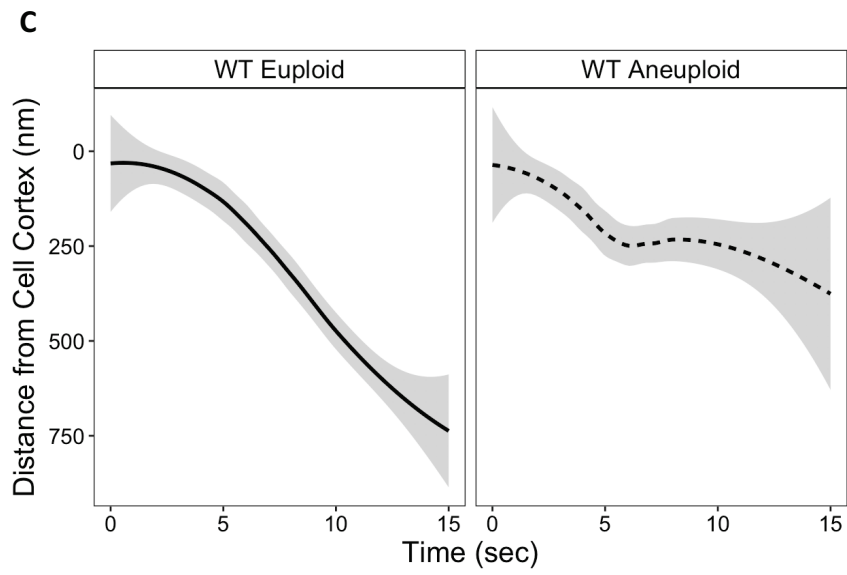
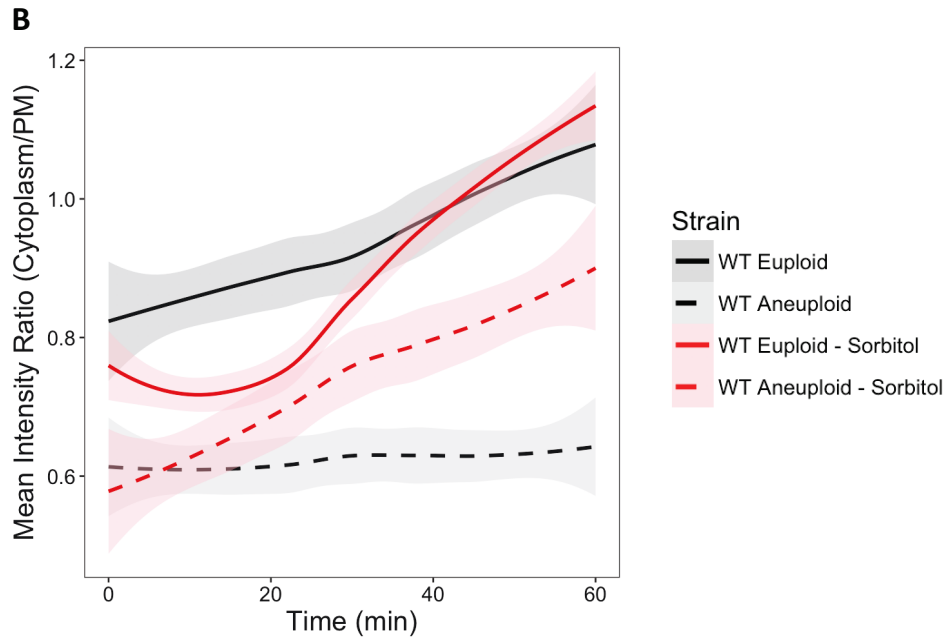
ingression force required for invagination of the endocytotic pit and slow down endocytosis. If turgidity was the obstacle, we hypothesized that addition of sorbitol would reduce the effective turgor pressure and rescue aneuploids from the endocytosis defect. Addition of 1M sorbitol to aneuploid cells significantly increased the rate of endocytosis in aneuploid cells. (Figure 12 B). Interestingly, euploid cells exhibited a slight initial delay in internalization of FM4-64 on the addition of sorbitol. This was probably due to the deviation from the turgor pressure ideal for euploid cells, reflecting that a tight regulation of turgidity is crucial for normal cell function.

We also examined the dynamics of a representative endocytotic protein Abp1p, an actin-binding protein that dynamically partitions between the plasma membrane and endocytotic vesicles and persists from endocytotic stage of invagination till post-scission (Kaksonen, Toret and Drubin 2005) . GFP-tagged Abp1p was monitored by time-lapse imaging and the distance moved by abp1-GFP patches (n = 20) into the cell interior from the cell cortex was found to be lower in aneuploid cells (Figure 12 C, D). Taken together, these results indicate that endocytosis in aneuploid cells is compromised.

Figure 12: Endocytosis is decreased in aneuploid cells. (A) Representative time-lapse micrographs of euploid, aneuploid and aneuploid cells with 1M sorbitol. Addition of 1M sorbitol to aneuploid cells results in an almost immediate internalization (*leftmost panel*). (B) Endocytosis dynamics measured as the ratio of mean fluorescence intensity ratio of FM4-64 in the cytoplasm to the plasma membrane (PM). Shaded regions denote the SE. (C) Distance travelled inwards from the cell cortex by abp1-GFP patches (n = 20). Distance

travelled by *abp1*-GFP patches is lower in aneuploid (dashed line) compared to euploid (solid line) strains. Shaded regions indicate standard error.





Discussion

In cancer, the ability of karyotypic heterogeneity to potentiate adaptability to existing drugs is a major obstacle to effective cancer therapeutics (Kreso, et al. 2013) (Fisher, Pusztai and Swanton 2013). If aneuploid cells, regardless of karyotypic complexity, exhibit a common signature or a predilection for particular genetic pathways, this so-called ‘vulnerability’ of aneuploids could be exploited to design a single therapeutic strategy that targets diverse karyotypes.

In this study, we have identified an aneuploidy associated transcriptional signature in budding yeast that is not biased towards specific karyotypes but is a global consequence of aneuploidy. Usually, in the analysis of aneuploid transcriptome profiles, direct copy number effects are accounted for by a n -fold downward adjustment for expression from the varied chromosome (Cromie, et al. 2016) (Hose, et al. 2015). This is not the most robust approach to studying aneuploid gene expression since the *trans*-effects of gene dosage are not considered. Moreover, most studies of aneuploidy to date have utilized aneuploid strains with specific karyotypes which fail to capture the intrinsic tumor heterogeneity (Torres, Sokolsky, et al. 2007) (Sheltzer, et al. 2012) (Cromie, et al. 2016). In our analysis, we forego the need for a copy number adjustment of gene expression by generating several karyotypically heterogeneous aneuploid populations, which are sufficiently large to exhibit a ploidy distribution similar to euploid populations.

Comparison of the resulting aneuploid population transcriptome to published gene expression datasets under different environmental stresses revealed that aneuploidy stress was distinctive, with the aneuploid population transcriptome highly similar to the gene expression profiles for hypo-osmotic and cell wall stresses. Additionally, one common

transcriptional effect previously observed in yeast disomic strains grown in batch cultures was the induction of the environmental stress response (ESR) (Torres, Sokolsky, et al. 2007), a common transcriptome signature observed in response to multiple harsh environmental transitions (Gasch, et al. 2000). Similar observations were made in the same group from the transcription signatures of trisomic *Arabidopsis thaliana* plants and mouse embryonic fibroblasts, with a hypothesis that this common feature of ESR induction was related to slow growth of aneuploids (Sheltzer, et al. 2012).

However, when the strains from Torres et al. (2007) were grown and evolved in chemostats instead of in batch culture, induction of the ESR was not observed, suggesting that ESR induction is highly dependent on culture conditions. Furthermore, in a growth assay of budding yeast aneuploid strains with random chromosome stoichiometries by Pavelka et al., enrichment of ESR genes was observed in only three out of five aneuploid strains and this enrichment did not correlate with growth rate (Pavelka, et al. 2010). Moreover, ESR was not activated in natural aneuploid strains grown in batch culture (Hose, et al. 2015). In a study of gene expression profiles of two budding yeast strains, disomic for either chromosome XV and XVI, Cromie et al. (2016) observed that the genes generally upregulated in the ESR had a lower expression in disomes and the downregulated ESR genes had a higher gene expression. In other words, the ESR was reversed in the aneuploid strains, both of which grew worse than a euploid in the same strain background, implying that the ESR induction is not a consequence of slow growth.

Similar to Cromie et al. (2016), we observed a strong negative correlation to conditions analogous to the directional response of the ESR previously associated with aneuploidy and proteotoxic stress, such as heat shock, oxidative stress, nitrogen depletion and long-

term DTT treatment, leading us to conclude that ESR induction and proteotoxic stress are not general responses to aneuploidy.

In addition to the aneuploidy transcriptome displaying a similarity to hypo-osmotic and cell wall stresses, aneuploid cells displayed phenotypes characteristic of an osmotic downshift and compromised cell wall, including drastic cell swelling, increased glycerol efflux, lower intracellular viscosity and a higher sensitivity to zymolyase. Interestingly, in a recent study, all but three disomes in budding yeast were found to display increased sensitivity to cell wall damaging agents such as Calcofluor white and Congo red. In addition, all but one disome showed decreased resistance to fluconazole, a drug which leads to cell membrane defects due to ergosterol depletion (Dodgson, et al. 2016). Together with our results, this suggests that cell wall defects might be a pervasive phenotype of aneuploidy.

Another consequence of aneuploidy we observed, was a measurable delay in bulk endocytosis. From our findings, a potential explanation that lends itself is that aneuploid cells possess cell wall defects which could provoke an indiscriminate uptake of organic osmolytes into the cell. This might then induce a hypo-osmotic stress response which could lead to both, a rapid influx of water into the cell and efflux of glycerol in an attempt to return to an isosmotic state. Cell swelling could subsequently cause an increase in turgor pressure, increasing the effective tension at the plasma membrane. Turgor pressure would enhance membrane tension and counteract the ingression forces of the endocytotic pit, effectively slowing down or disrupting endocytosis. Endocytosis plays an integral role in cellular homeostasis and is known to govern cell proliferation, establishment of polarity and nutrition uptake (Di Fiore and Zastrow 2014). Defects in endocytosis can have

profound consequences on cell physiology, and endocytosis is disrupted in several diseases, including certain types of cancer (McMahon and Boucrou 2011). For instance, genes encoding some of the proteins that participate directly in the clathrin coat during early stages of endocytosis have been identified as targets of chromosomal rearrangements in human hematopoietic malignancies (Floyd and Camilli 1998).

Cell wall formation is known to rely on endocytosis and protein trafficking. Studies of the cell wall stress sensor, Wsc1p, in budding yeast mutants with endocytosis-defects revealed that when endocytosis was blocked, the localization of Wsc1 was altered, which resulted in increased sensitivity to perturbations in cell wall biosynthesis by the $\beta(1-3)$ glucan inhibitor, caspofungin (Piao, Machado and Payne 2007). This would imply that an endocytosis defect might provide a feedback that further compromises the cell wall and create a vicious cycle.

However, in our study, cell swelling is not observed after propagation of these cells over several cell cycles, suggesting that aneuploid cells might possess a mechanism by which they can overcome this stress. This, however, does not diminish the potential therapeutic contributions since certain mutations in the endocytosis or cell wall integrity pathways might exaggerate this aneuploidy stress and result in a universal feature that can be drug-targeted. In fact, a recent genome-wide screen for aneuploids carrying homozygous gene deletions which impair the fitness of heterogeneous aneuploid populations compared to euploid populations carrying the same gene deletion, was performed in our lab (Hung-Ji Tsai, unpublished results). Indeed, genes identified by this screen are known to play a role in plasma membrane turnover and vesicle trafficking. In conclusion, the work presented in this thesis in conjunction with the results of the genome-wide screen for mutations that

compromise aneuploid fitness, could offer further insight into the molecular mechanisms that govern aneuploidy.

References

- Anders, S, P T Pyl, and W Huber. "HTSeq--a Python framework to work with high-throughput sequencing data." *Bioinformatics* 31, no. 2 (2015): 166-9.
- Basu, Roshni, Emilia Laura Munteanu, and Fred Chang. "Role of turgor pressure in endocytosis in fission yeast ." *Molecular Biology of the Cell* 25, no. 5 (2014): 679-687.
- Birchler, J A. "Reflections on studies of gene expression in aneuploids." *Biochemical Journal* 462, no. 2 (2010): 119-123.
- Chen, G, et al. "Targeting the Adaptability of Heterogeneous Aneuploids." *Cell* 160, no. 4 (2015): 771-784.
- Cromie, G. A., Z. Tan, M. Hays, E. W. Jeffery, and A. M. Dudley. "Dissecting Gene Expression Changes Accompanying a Ploidy-Based Phenotypic Switch." *G3: Genes, Genomes, Genetics* 7, no. 3 (2016).
- Dodgson, Stacie, et al. "Chromosome-Specific and Global Effects of Aneuploidy in *Saccharomyces cerevisiae*." *Genetics* 202, no. 4 (2016): 1395-409.
- Garcia, Raul, Jose M Rodríguez-Peña, Clara Bermejo, and Javier Arroyo. "The High Osmotic Response and Cell Wall Integrity Pathways Cooperate to Regulate Transcriptional Responses to Zymolyase-induced Cell Wall Stress in *Saccharomyces cerevisiae*." *Journal of Biological Chemistry* 284, no. 16 (2009).
- Gasch, A P, et al. "Genomic expression programs in the response of yeast cells to environmental changes." *Molecular Biology of the Cell* 11, no. 12 (2000): 4241-4257.
- Giam, Maybelline, and Giulia Rancati. "Aneuploidy and chromosomal instability in cancer: a jackpot to chaos." *Cell Division* 10, no. 3 (2015).
- Haidekker, M A, and E A Theodore. "Molecular rotors - fluorescent biosensors for viscosity and flow." *Organic and Biomolecular Chemistry* 5, no. 11 (2007): 1669-1678.
- Hohmann, Stefan. "Osmotic Stress Signaling and Osmoadaptation in Yeasts ." *Microbiology and Molecular Biology Reviews* 66, no. 2 (2002): 300-372.
- Hose, James, Chris Mun Yong, Maria Sardi, Wang Zhishi, Micahel Newton, and Audrey P Gasch. "Dosage compensation can buffer copy-number variation in wild yeast." *eLife* 4 (2015): e05462.
- Kim, D, B Langmead, and S. L. Salzberg. "HISAT: a fast spliced aligner with low memory requirements. ." *Nature Methods* 12 (2015): 357-360.
- Klipp, Eda, Bodil Nordlander, Rolan Kruger, Peter Genemark, and Stefan Hohmann. "Integrative model of the response of yeast to osmotic shock." *Nature Biotechnology* 3, no. 8 (2005).
- Kuimova, Marina K, Gokhan Yahioğlu, James A Levitt, and Klaus Suhling. "Molecular Rotor Measures Viscosity of Live Cells via Fluorescence Lifetime Imaging." *Journal of the American Chemical Society* 130, no. 21 (2008): 6672-6673.
- Langmead, Ben, and Steven L Salzberg. "Fast gapped-read alignment with Bowtie 2." *Nature Methods* 9, no. 4 (2012): 357-359.

- Levin, David E. "Cell Wall Integrity Signaling in *Saccharomyces cerevisiae*." *Microbiology & Molecular Biology Reviews* 69, no. 2 (2005): 262-291.
- Li, Heng, et al. "The Sequence Alignment/Map format and SAMtools." *Bioinformatics* 25, no. 16 (2009): 2078-2079.
- Love, M. I., W. Huber, and S. Anders. "Moderated estimation of fold change and dispersion for RNA-seq data with DESeq2." *Genome Biology* 15, no. 50 (2014).
- Miermont, Agnes, et al. "Severe osmotic compression triggers a slowdown of intracellular signaling, which can be explained by molecular crowding." *Proceedings of the National Academy of Sciences of the United States of America* 110, no. 14 (2013).
- Mourao, Marcio A, Joe B Hakim, and Santiago Schnell. "Connecting the Dots: The Effects of Macromolecular Crowding on Cell Physiology." *Biophysical Journal* 107 (2014): 2761-2766.
- Mulla, Wahid, Jin Zhu, and Rong Li. "Yeast: A simple model system to study complex phenomena of aneuploidy." *FEMS Microbiology Reviews* 38, no. 2 (2013): 201-212.
- Musacchio, Andrea, and Edward D Salmon. "The spindle-assembly checkpoint in space and time." *Nature Reviews Molecular Biology* 8 (2007): 379-393.
- Oromendia, A B, and Angelika Amon. "Aneuploidy: implications for protein homeostasis and disease." *Disease Models & Mechanisms* 7 (2014): 15-20.
- Oromendia, Ana B, Stacie E Dodgson, and Angelika Amon. "Aneuploidy causes proteotoxic stress in yeast." *Genes and Development* 26, no. 24 (2012): 2696-2708.
- Pavelka, Norman, et al. "Aneuploidy confers quantitative proteome changes and phenotypic variation in budding yeast." *Nature* 468, no. 7321 (2010): 321-5.
- Pavelka, Norman, Giulia Rancati, and Rong Li. "Dr. Jekyll and Mr. Hyde: Role of Aneuploidy in Cellular Adaptation and Cancer." *Current Opinions in Cell Biology* 22, no. 6 (2010): 809-815.
- Piao, Hai Lan, Iara M P Machado, and Gregory S Payne. "NPFXD-mediated Endocytosis Is Required for Polarity and Function of a Yeast Cell Wall Stress Sensor." *Molecular Biology of the Cell* 18, no. 1 (2007): 57-65.
- Rancati, Giulia, et al. "Aneuploidy underlies rapid adaptive evolution of yeast cells deprived of a conserved cytokinesis motor." *Cell* 135, no. 5 (2008): 879-893.
- Selmecki, Anna, Anja Forche, and Judith Berman. "Aneuploidy and Isochromosome Formation in Drug-Resistant *Candida albicans*." *Science* 313, no. 5785 (2006): 367-370.
- Seshan, Venkatraman E, and Adam Olshen. *DNACopy: DNA copy number data analysis*. 2016.
- Sheltzer, Jason M, E M Torres, M J Dunham, and Angelika Amon. "Transcriptional consequences of aneuploidy." *Proceedings of the National Academy of Sciences of the United States of America* 109 (2012): 12644-12649.
- Siegel, J J, and Angelika Amon. "New insights into the troubles of aneuploidy." *Annual Review of Cell and Developmental Biology* 28 (2012): 189-214.
- Stingele, S., G. Stoehr, K. Peplowska, J. Cox, M. Mann, and Z. Storchova. "Global analysis of genome, transcriptome and proteome reveals the response to aneuploidy in human cells." *Molecular Systems Biology* 8, no. 608 (2012).

- Strimmer, Korbinian. "fdrtool: a versatile R package for estimating local and tail area-based false discovery rates." *Bioinformatics* 24, no. 12 (2008): 1461-1462.
- Tang, Yun Chi, Bret R Williams, Jake J Siegel, and Angelika Amon. "Identification of Aneuploidy-Selective Antiproliferation Compounds." *Cell* 144, no. 4 (2011): 499-512.
- Toh, Tze Hsien, et al. "Implications of FPS1 deletion and membrane ergosterol content for glycerol efflux from *Saccharomyces cerevisiae*." *FEMS Yeast Research* 1, no. 3 (2001): 205-211.
- Torres, E M, et al. "Effects of aneuploidy on cellular physiology and cell division in haploid yeast." *Science* 317, no. 5840 (2007): 916-924.
- Torres, E M, et al. "Identification of aneuploidy-tolerating mutations." *Cell* 143, no. 1 (2010): 71-83.
- Torres, E M, M Springer, and Angelika Amon. "No current evidence for widespread dosage compensation in *S.cerevisiae*." *Elife* 5 (2016): e10996.

Anjali Rebecca Nelliat

701 Cathedral Street
Baltimore, MD 21201
(562) 387-6325
anjali.nelliat@gmail.com

Education **M.S in Chemical and Biomolecular Engineering,** August 2015 - Present
Johns Hopkins University, Baltimore, MD
B.Tech in Chemical Engineering, July 2011 - May 2015
National Institute of Technology Karnataka, India

Core Skills

- Standard molecular biology protocols and yeast genetics.
- High-throughput screening (HTS) and subsequent HTS data analysis.
- Confocal/wide-field microscopy and design of image analysis pipelines.
- Mathematical modeling and statistical analysis of biological data.
- Downstream analysis of next generation sequencing (NGS) data.
- Design of Experiments (DoE) methods.
- HPLC, SEM.

Technical Skills *Programming Languages:* R, MATLAB, C++, Unix Shell.
Software: COMSOL, ImageJ, SAMtools, bowtie2, and other NGS analysis tools.

Experience **Graduate Student Researcher** December 2015 - Present
Center for Cell Dynamics, Johns Hopkins University
Project: Investigating the global effects of aneuploidy on genome evolution and cell physiology.

- Performed high-throughput genetic screen to study gene essentiality in aneuploids and mined the HTS data.
- Designed and conducted a high-throughput microscopy assay and developed an image processing pipeline to study population heterogeneity and adaptation.
- Formulated and implemented an effective mathematical model for analysis of aneuploid population fitness based on a high-throughput genetic screen.
- Conducted data analysis of RNA-Seq and DNA-Seq data from aneuploid populations and performed functional assays based on the results to study dynamic cellular processes.

Research Assistant August 2014 - May 2015
National Institute of Technology Karnataka, India
Project: Synthesis of cellulosic bionanocomposites using bacterial cellulose for applications in wound healing.

- Using brewery waste as an alternate low-cost carbon source, optimized production of bacterial cellulose.
- Lowered the biological oxygen demand (BOD) of brewery waste by greater than 99%, to well within permissible disposal limits within a fortnight of cell growth.

Summer Research Assistant May 2014 - July 2014
Nanyang Technological University, Singapore
Project: Designing liposomes for treatment of inflammatory ocular disorders.

- Achieved up to 60 days of sustained drug release from liposomes *in vitro*.
- Successfully resolved the issue of initial burst release.

Undergraduate Researcher September 2013 - May 2014
National Institute of Technology Karnataka, India
Project: Optimization of L-Asparaginase production from endophytic fungi.

- Effectively used DOE methods such as the Plackett-Burman design for optimization of growth media.
- Responsible for the initial optimization of carbon and nitrogen sources.

Presentations **Nelliath, A.R.**, Tsai, H., Li, R. (2016, December). *Quantitative fitness analysis of cell-to-cell heterogeneity in aneuploid populations*. Poster presented at the American Society for Cell Biology Meeting, San Francisco, CA.

Abstracts **Nelliath, A.R.**, Tsai, H., Li, R. (2016). Quantitative fitness analysis of cell-to-cell heterogeneity in aneuploid populations. *Mol. Biol. Cell* 2016, 27(25), page 118.

Awards ASCB 2016 Graduate Student Travel Award October 2016
 Johns Hopkins ChemBE Master Essay Scholarship July 2016
 St. Aloysius Meritorious Student Award July 2011

Affiliations *Graduate Member* July 2016 - Present
 American Society for Cell Biology (ASCB)
Creative Head, Student Chapter July 2014 - May 2015
 Indian Society for Technical Education (ISTE)
Editor August 2013 - May 2015
 NewsWagon - University Newspaper
Joint Convener July 2014 - May 2015
 EngiConnect - A state-wide initiative to introduce high school students to engineering.

References Dr. Rong Li
 Professor, Department of Cell Biology
 Johns Hopkins University School of Medicine
 Baltimore, MD 21205
 Rong@jhu.edu

Dr. Michael Schatz
 Associate Professor, Department of Computer Science and Biology
 Johns Hopkins University
 Baltimore, MD 21218
 mschatz@cs.jhu.edu